

## Electronic and atomic structure of amorphous carbon

J. Robertson

*Central Electricity Research Laboratories, Central Electrical Generating Board, Leatherhead,  
Surrey KT22 7SE, United Kingdom*

E. P. O'Reilly

*Department of Physics, University of Surrey, Guildford, Surrey, GU2 5XH, United Kingdom*

(Received 22 August 1986)

The electronic structure of amorphous carbon and hydrogenated amorphous carbon (*a*-C:H) has been investigated through calculations on a number of model structures containing different configurations of  $sp^2$  and  $sp^3$  sites. We find that the most stable arrangement of  $sp^2$  sites is in compact clusters of fused sixfold rings, i.e., graphitic layers. The width of the optical gap is found to vary inversely with the  $sp^2$  cluster size, and the  $\sim 0.5$ -eV optical gap of evaporated amorphous carbon is found to be consistent with a model of disordered graphitic layers of about 15 Å in diameter, bounded by  $sp^3$  sites. It is argued that *a*-C forms such finite clusters in order to relieve strain. It is then shown that the 1.5–2.5-eV optical gap of *a*-C:H is unusually small and requires that both its valence and conduction band consist of  $\pi$  states on  $sp^2$  sites and that these sites must also be significantly clustered, such as in graphitic clusters containing four or more rings. In other words, the optical gap of both *a*-C and *a*-C:H depends on their degree of medium-range order, rather than just on their short-range order as is the case in most amorphous semiconductors. We have also studied the nature of states away from the gap in order to interpret the photoemission data and the carbon 1s core-level absorption spectra. The nature of defects and midgap states is discussed, and it is predicted that the defect density decreases with increasing band gap. Finally it is argued that the doping of *a*-C:H by group-III and -V elements proceeds via a substitution mechanism, as in *a*-Si:H, in spite of the coordination disorder present in *a*-C:H. Doping is also expected to be accompanied by an increase in gap states, as in *a*-Si:H.

### I. INTRODUCTION

The properties of amorphous carbon depend strongly on their temperature of preparation and hydrogen content. There are broadly two forms of amorphous carbon, the black semiconducting films prepared by evaporation or sputtering which we shall call *a*-C, and the hydrogenated amorphous carbon (*a*-C:H) prepared by plasma deposition of hydrocarbons such as ethylene. The latter has recently attracted attention for its hardness, chemical inertness, optical transparency, and its ability to be doped.<sup>1,2</sup> The structure of these amorphous carbons has been greatly debated because of carbon's ability to form both threefold coordinate ( $sp^2$ ) sites, as in graphite, and fourfold ( $sp^3$ ) sites, as in diamond. A variety of techniques<sup>3–7</sup> suggest that *a*-C itself is predominantly  $sp^2$  bonded with an optical gap of 0.4–0.7 eV and that hydrogenation introduces many  $sp^3$  sites and increases the gap to 1.6–2.7 eV.<sup>7–11</sup>

Because of the  $sp^2$  sites, the electronic structure of amorphous carbon and the effect of disorder is very different to that of *a*-Si. For a group-IV element at an  $sp^3$  site, each of the four valence electrons lies in an  $sp^3$  hybrid which then forms a  $\sigma$  bond with a neighbor.<sup>12</sup> At an  $sp^2$  site, only three of these electrons are used in  $\sigma$  bonds, the fourth enters a  $\pi$  orbital which lies normal to the  $\sigma$  bonding plane. The importance of the  $\pi$  states is that they are only weakly bonding so that they usually lie

closest to the Fermi level  $E_F$ . They will therefore form both the valence- and conduction-band states in *a*-C and also, as we shall see, in *a*-C:H. Now, the effect of disorder in  $sp^3$  bonded systems has been thoroughly studied and it is known that the optical gap persists in *a*-Si, provided that Si atoms retain their tetrahedral coordination.<sup>12,13</sup> In contrast, the effect of disorder in  $\pi$ -bonded systems has been little studied. We first note that the presence of a gap in *a*-C is very significant, given that graphite itself has no gap. Clearly, the nature of the disorder is to allow a gap to open up rather than to eliminate it.<sup>14</sup>

This paper is organized as follows: Sec. II describes the methods used in the electronic structure calculation. In Sec. III the origin of the gap is analyzed in terms of the interaction of  $\pi$  states, and we then discuss in Sec. IV the constraints this places on the possible atomic structure of *a*-C. Section V contains a similar discussion on the size of the gap in *a*-C:H and the degree of saturation of  $sp^2$  sites (conversion to  $sp^3$  sites) by hydrogen. General aspects of the electronic structure are discussed in Sec. VI, while the defects and nature of the doping mechanism in *a*-C:H are discussed in Secs. VII and VIII.

### II. INITIAL CALCULATIONS

In this paper we describe the electrons by a tight-binding Hamiltonian, which uses an  $sp^3$  basis set and retains only first-neighbor interactions and some second-

TABLE I. Interaction parameters in eV for C—C and C—H bonds. Energies are referred to  $E_F$  of graphite, lying 4.7 eV below the vacuum level.

	$E(s)$	$E(p)$	$E(s^*)$				
C	-5.35	0.45	14.0				
H	-2.3						
	$V(ss)$	$V(sp)$	$V(p\sigma)$	$V(p\pi)$	$V(p_z\pi)$	$V_2(p_z\pi)$	$V(s^*p)$
C—C	-4.55	5.2	5.45	-1.6	-2.9	0.15	4.5
C—H	-7.5	8.9					

neighbor interactions. The parameters used are given in Table I and were found by fitting existing band structures<sup>15–17</sup> and the experimental photoemission<sup>18,19</sup> and optical gap.<sup>20</sup> The interaction parameters were chosen to provide a good modeling of the band-edge states of  $a$ -C and also to give the correct overall band widths. For simplicity a common set of parameters were used for both  $sp^3$  and  $sp^2$  sites (although if bond alternation occurred, we would need to allow  $\pi$  interactions to vary with bond length). However, the  $\pi$  interactions are carefully described, as earlier.<sup>21</sup> The  $\pi$  interaction between two  $\pi$  states, denoted  $V(p_z\pi)$ , must be larger than that between two  $p\sigma$  states in order to fit the overall  $\pi$  band width of graphite. Also, a second-neighbor  $\pi$  interaction  $V_2(p_z\pi)$  is included, unlike in the earlier calculations.<sup>14</sup> This interaction produces the observed asymmetry of widths of the valence  $\pi$  and conduction  $\pi^*$  bands. With the common orbital energies, it also has the effect of giving the correct alignment of  $\sigma$  and  $\pi$  bands, which is needed for confidence in our later predictions of the character of the band-edge states in  $a$ -C:H.

The resulting band structures for a single layer of graphite and for diamond are shown in Fig. 1, and their density of states (DOS) is shown in Figs. 2(a) and 2(b). We see that a single layer of graphite is a zero band-gap semiconductor because the  $\pi$  bands touch at  $E_F$  at the  $K$  point. The peaks in the  $\pi$  DOS arise from states around the  $M$  point. The  $\sigma$  states of graphite and diamond lie well away from  $E_F$  and the graphite  $\pi$  states lie within the

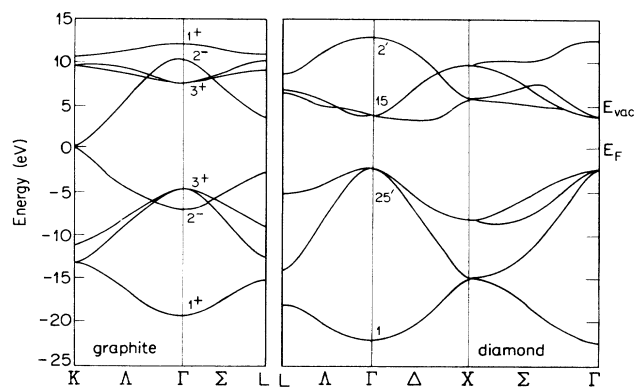


FIG. 1. Band structure of (a) a single layer of graphite, (b) diamond, and referred to  $E_F$  of graphite.

$\sigma$  gap, which is a general feature of all  $\pi$  bonded systems. Interestingly, the difference in the work functions of graphite<sup>16</sup> (4.7 eV) and of diamond [experimental 6.9 eV (Ref. 22), calculated 7.25 eV], is fairly well reproduced by our parameters, in spite of simple treatment of the work-function concept in tight-binding theory.<sup>23</sup> The lineup of their conduction bands, as seen in the carbon 1s x-ray

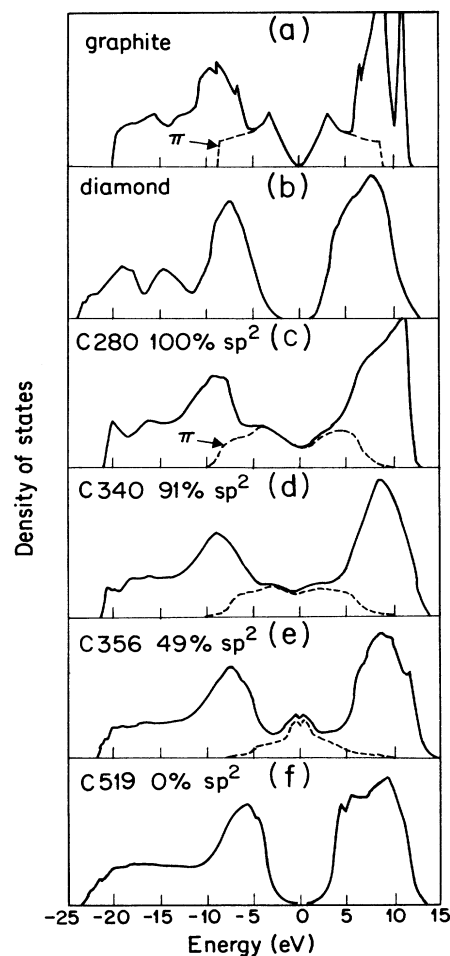


FIG. 2. Local density of states of graphite, diamond, and of the four random networks of Beeman *et al.* (Ref. 5), calculated by the recursion method.

near-edge spectra (XANES), is also reproduced with fair accuracy (a 3.0-eV calculated versus a 4-eV experimental separation between the onset of transitions in graphite and diamond).<sup>7</sup> Our calculations for graphite omit the strongly dispersive interlayer states derived from carbon 3s orbitals and found at  $E_F + 4$  eV and above.<sup>24-26</sup>

The parameters for the C—H bond were fitted to the molecular energy levels calculated for methane.<sup>27</sup> They are also consistent with experimental photoemission and XANES data.<sup>28,29</sup>

To study the electronic structure of random networks, the recursion method<sup>30</sup> is used to calculate the local density of states at selected sites. Twenty levels of the continued fraction are retained and the orbital character of any peak is found by analyzing the poles of the Green's function.<sup>31</sup> The recursion method tends to round off the DOS, as can be seen in results for graphite and diamond, Figs. 2(a) and 2(b).

Figures 2(c)–2(f) shows the local DOS averaged over six sites at the middle of three possible random networks of *a*-C, which contain 100%, 91%, 51%, and 0% of  $sp^2$  hybridized sites, respectively.<sup>5</sup> The first network consists of warped graphitic layers but contains a high proportion of odd-membered rings of bonds. The last network containing 100%  $sp^3$  sites is the Polk model, scaled to *a*-C. We note that all three networks containing  $sp^2$  sites have a finite DOS at  $E_F$ .<sup>14</sup> This result immediately refutes one naive idea about *a*-C, that the mere presence of  $sp^3$  sites is sufficient to open up a gap. We shall now show that the  $sp^2$  sites must be spatially correlated to produce a gap even in the presence of  $sp^3$  sites, and indeed can even produce a gap with no  $sp^3$  sites present.

### III. ANALYSIS OF THE $\pi$ STATES

The existence of a gap in  $\pi$  states can be analyzed by neglecting the  $\sigma$  states entirely, because  $\pi$  states lie closer to  $E_F$  and because, to first order, local symmetry decouples them from the  $\sigma$  states. A key feature of the  $\pi$  states in Fig. 2 is that they are half filled, so that creating a gap in their spectrum at  $E_F$  will tend to lower the total  $\pi$  electron energy per atom,  $E_{\text{tot}}$ , and thereby stabilize the new structure. Thus, the driving force giving the gap in *a*-C is that this tends to lower the  $\pi$  electron energy. This is opposed by the  $\sigma$  backbone whose energetics can be described by a valence force field of bond-stretching and bond-bending forces. Stated thus, it is clear that the gap will depend primarily on the concentration and disposition of the  $\pi$  states, and only indirectly on other factors such as hydrogen content.

To analyze the  $\pi$  states, they are represented by a Hückel Hamiltonian. This is a one-electron tight-binding model which retains only the  $\pi$  orbitals and the nearest-neighbor interactions between them,  $\beta = V(p_z\pi)$ . The orbital self-energy  $E_p$  is set to zero in this section. This model maps the network of  $sp^2$  and  $sp^3$  sites into a sparser network of only  $\pi$  states, which in practice consists of a series of separate clusters. We expect each cluster to behave like the analogous organic molecule whose properties are well known.<sup>32,33</sup> The most stable structure is that with the lowest  $E_{\text{tot}}$ , values of which are collected

in Table II. A related analysis of carbon clusters in the Hückel approximation has been carried out by Hoffman<sup>34</sup> and by Pitzer and Clementi.<sup>35</sup>

Consider first some small clusters. The simplest cluster is a pair of adjacent  $\pi$  sites. These interact to form an occupied  $\pi$  and an empty  $\pi^*$  state, with energies [Fig. 3(a)]

$$E = \pm\beta \cos\phi . \quad (1)$$

The orbitals tend to orient parallel, with the dihedral angle  $\phi=0$ , to minimize the total  $\pi$  energy  $E_{\text{tot}}=2\beta$ , or normalized per site and in units of  $\beta$ :

$$E_{\text{tot}} = 1 , \quad (2)$$

and form a "double bond" C=C. This also maximizes the gap

$$E_g = 2|\beta| . \quad (3)$$

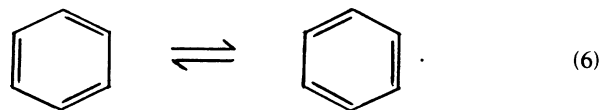
Now consider an isolated ring with  $N$  vertices. Rings with  $N=3,4$  distort the  $\sigma$  backbone too much to be stable and are ignored. If the ring is planar and all bonds have the same length, then the eigenvalues are

$$E_n = 2\beta \cos \left[ \frac{2\pi n}{N} \right], \quad n = 1, 2, \dots, N . \quad (4)$$

Figure 3(b) shows that rings of  $N=5, 7$ , and 8 give half-filled levels. Only  $N=6$ , benzene, has all levels lying well away from  $E=0$ . This produces a stable structure and strongly favors sixfold rings. Furthermore,

$$E_{\text{tot}} = \frac{4}{3} , \quad (5)$$

which is  $\frac{1}{3}$  more stable than three separate double bonds. Qualitatively, this is often attributed to the resonance





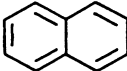
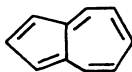
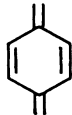
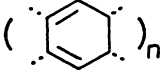
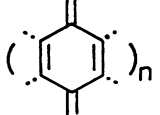
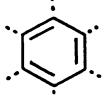
This stability is referred to as Hückel's rule of aromatic stability, that planar rings with  $4N+2$   $\pi$  electrons are more stable than other rings or equivalent acyclic systems. Also, for  $N=6$ ,

$$E_g = 2|\beta| . \quad (7)$$

Planar rings are favored for  $N=6$  to maximize the interaction between adjacent  $\pi$  orbitals. However, for  $N=8$  (octatetracene), there are two half-filled levels at  $E_F$  so the system undergoes a Jahn-Teller distortion into a tub structure which produces four almost independent double bonds.<sup>32</sup>

A qualitative distinction is often drawn between the  $\pi$  bond in ethylene and the  $\pi$  bonds in benzene or graphite. The  $\pi$  bond in ethylene can be represented as an electron pair localized between two centers—a two-electron, two-center bond of Lewis form, as are the  $\sigma$  bonds. In contrast, the six  $\pi$  electrons of benzene are shared between six equivalent C—C bonds, and not three bonds as in either of the resonance structures in (6). A delocalized descrip-

TABLE II.  $\pi$  energy per site for various  $sp^2$  bonding configurations.

Group	Name	$E_{\text{tot}}/\beta$
	Polyacetylene	1
	Benzene	1.333
	Naphthalene	1.368
	Azulene	1.336
	Quinoid	1.240
	Polybenzoid	1.403
	Polyquinoid	1.216
	Graphite	1.616

tion of benzene's  $\pi$  bonding is inevitable and such systems are called conjugated.

A large variety of larger clusters can be formed by fusing rings together or fusing double bonds and rings. The more probable configurations are those with the highest  $E_{\text{tot}}/\beta$ .  $E_{\text{tot}}$  values are displayed for various configurations in Fig. 4 and Table II, and these can usually be relat-

ed to the behavior of  $E_g$  shown in Figs. 3 and 5. Their behavior is described by the following four rules.

(1) For a system of only even-membered rings and linear chains and in the nearest-neighbor approximation, the eigenvalue spectrum is found to be symmetric about  $E = 0$ . For odd  $N$  there is always one state at  $E = 0$  [e.g., Fig. 3(c)], which destabilizes the cluster. Thus a gap can only exist when the total number of sites  $N$  is even, and indeed Fig. 4 shows that  $E_{\text{tot}}$  is larger for even  $N$  than for odd  $N$ .

(2) Sixfold rings are favored, whether isolated or fused with others—for example,  $E_{\text{tot}}$  of a pair of sixfold rings is greater than of a 5-7 ring combination (Table II). This is because odd rings still tend to fill in the gap at  $E_F$ . This is seen most clearly in the local density of states [Figs. 3(e)] of a "quadrupole" of two fivefold and sevenfold rings in an otherwise infinite graphite layer. (This configuration is created by a "T1" bond flip<sup>36</sup> in a perfect layer.)

(3) Closed rings of  $\pi$  states are favored. For example, if an extra  $\pi$  site is added at the 1 and 4 positions of a benzene ring, a quinoid structure is created (8). Its  $E_{\text{tot}}$  of 1.24 is less than that of a benzene ring and one double bond separately, 1.25. This is attributed to the absence of a resonance akin to (6),



Calculations also support this inequality for large clusters. This suggests that aromatic rings with "spurs" would tend to dissociate into closed rings plus double bonds, if the  $\sigma$  network allows this. Quinoid structures also tend to have narrower gaps, e.g., (8) has  $E_g = 0.61 |\beta|$  compared to  $2 |\beta|$  for benzene.

(4) Compact clusters of fused sixfold rings are favored over rows of rings. The dependence of  $E_{\text{tot}}/\beta$  on the number of rings  $M$  is shown in Fig. 4 and its value for the most compact clusters is consistently greater than that for rows. These results indicate that large carbon clusters will tend to be graphitic.

Figure 5 shows the variation of the gap for two types of clusters. Firstly  $E_g$  varies rather unevenly with ring number for compact clusters (because of their changing symmetry) but eventually follows the trend:

$$E_g = 2 |\beta| M^{-0.5} . \quad (9)$$

Less compact clusters have smaller gaps. Figure 5 also shows that for a linear row of rings,  $E_g$  ultimately decreases rapidly according to

$$E_g \propto M^{-2} \quad (10)$$

at large  $M$ . Other clusters lie between these limits. We

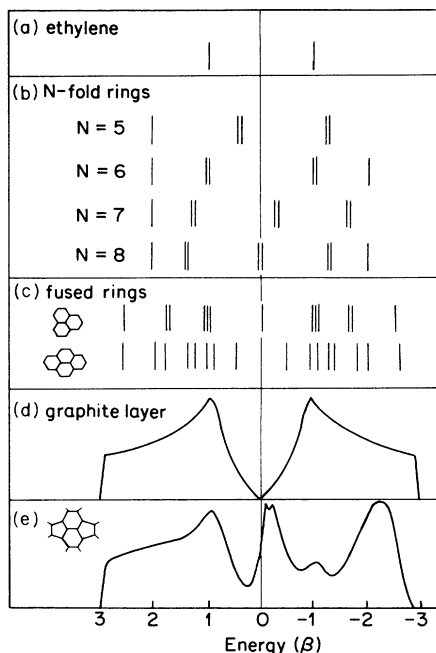


FIG. 3.  $\pi$ -state spectra of (a) ethylene, (b) planar rings with  $N=5-8$ , (c) three fused sixfold rings, and four fused sixfold rings, (d) single graphite layer, and (e) layer containing two fivefold and two sevenfold rings.

expect the more compact clusters, with wider gaps, to dominate the properties of  $a$ -C in practice, because of their greater  $E_{\text{tot}}/\beta$ .

In  $a$ -C:H, it is also possible that  $sp^2$  sites are arranged in  $\pi$  bonded chains, analogous to  $C_NH_{N+2}$ . If their  $\pi$  orbitals are all parallel, the eigenvalues are

$$E = 2\beta \cos \left[ \frac{\pi n}{N+1} \right], \quad n = 1, 2, \dots, N. \quad (11)$$

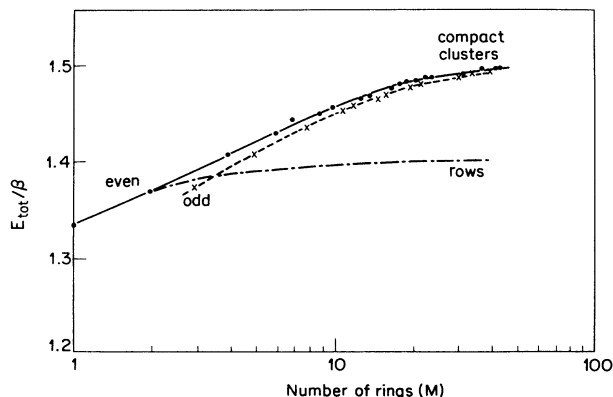


FIG. 4.  $\pi$  electron energy per atom for clusters of fused sixfold rings, both compact and linear, in units of  $\beta$ . The compact clusters with even and odd numbers of atoms are distinguished.

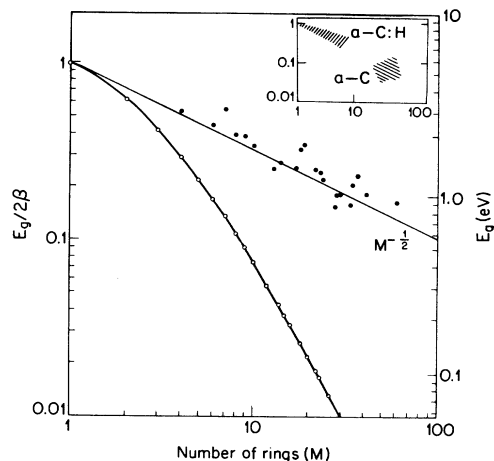


FIG. 5. Minimum gap for compact (upper) and linear (lower) clusters of fused sixfold rings. Inset shows probable cluster sizes found in  $a$ -C and  $a$ -C:H.

For  $N$  even, the two states closest to  $E_F$  lie at  $E \approx \pm \beta\pi/N$ , giving

$$E_g \approx 2\beta\pi/N \quad (12)$$

for large  $N$ . Dihedral disorder is easier than in the ring structures, and acts to decrease the gap. For  $N \geq 20$ , the gap is so narrow that a Peierls distortion occurs, and the bonds alternate in length, as in polyacetylene.<sup>33</sup> It is not anticipated that this limit is reached in  $a$ -C:H.

The Hückel theory arguments used in this section are generally sufficient to understand the behavior of  $\pi$  electrons in amorphous carbon. The major problem is that it is a one-parameter theory. It is found that the optimum value of  $\beta$  for band-structure energies and optical gaps is that fitted to the  $\pi$  bands of graphite,  $\beta = -2.9$  eV (Table I). This also gives a fair description of the  $\pi \rightarrow \pi^*$  optical transitions in ethylene and benzene, if the various singlet and triplet excitations are all averaged. However, this value of  $\beta$  overestimates total energies, and a value of  $\beta = -1.4$  eV must be used. This was found by averaging  $\pi$  bond energies in simple molecules.<sup>32</sup> A similar problem is found in  $\sigma$  bonded systems if only a single bond energy parameter  $V_2$  is used to parametrize both gaps and total energies.<sup>37</sup>

#### IV. PROPERTIES OF AMORPHOUS CARBON

In order to apply these results to  $a$ -C we first review previous structural work which suggests that it consists of  $\sim 95\%$   $sp^2$  sites and the possibility that these may form disordered graphitic islands of 15–20 Å diameter. We then show that this model is consistent with the observed band gap, and suggest why “islands” should exist.

Electron-energy-loss<sup>7,38</sup> and XANES (Refs. 7 and 39) spectra suggest that low-temperature deposited  $a$ -C is  $\sim 95\%$   $sp^2$ . Magic-angle spinning  $^{13}\text{C}$  nuclear magnetic resonance (NMR) would provide a direct measurement of the  $sp^2$  concentrations—but unfortunately the signal is presently too weak to be measured in unhydrogenated ma-

terial.<sup>9</sup> Diffraction studies over the years have been much more contentious.<sup>6,40–45</sup> Kakinoki *et al.*<sup>41</sup> proposed a 50%  $sp^2$ , 50%  $sp^3$  model of  $a$ -C, but most others suggest a much higher proportion of  $sp^2$  sites. The radial distribution functions (rdf's) and density of a continuous-random-network (CRN) model of Beeman *et al.*<sup>5</sup> containing 91%  $sp^2$  sites, fitted the experimental rdf better than models containing 100%  $sp^2$  or 50%  $sp^2$  sites. Mildner and Carpenter<sup>6</sup> proposed that their glassy carbon contained  $\sim 95\%$  sites. However, it should be noted that the structure of  $a$ -C depends strongly on its deposition or anneal temperature, and that above 1000 °C the (002) interlayer diffraction peak of graphite at  $\sim 1.88 \text{ \AA}^{-1}$  becomes strong and sharp in the structure factor, so that a true microcrystalline model might be more appropriate for their high-temperature material. Indeed, the structure factor of some "glassy carbon" has been accurately fitted by a strained graphite model.<sup>46</sup> However, one should note that models of (low-temperature)  $a$ -C will still tend to possess a (002) peak, as some medium-range order is inevitable in layered structures.

Some of the most useful information on  $a$ -C comes from its Raman spectra,<sup>4,47,48</sup> which shows a broad asymmetric peak at  $1540\text{--}1580 \text{ cm}^{-1}$ , close to the  $1575 \text{ cm}^{-1}$  Raman line of graphite and the  $1623\text{-cm}^{-1}$  frequency of ethylene, but much higher than the  $1330\text{-cm}^{-1}$  line of diamond. Interestingly, a subsidiary peak around  $1350 \text{ cm}^{-1}$  is found to grow in as  $a$ -C is annealed above 300 °C.<sup>4</sup> It is also seen in infrared spectra.<sup>49</sup> This peak is not due to  $sp^3$  sites, as heating tends to cause graphitization, if anything. Rather, it is attributed to the intralayer "disorder mode" seen in microcrystalline graphite.<sup>50,51</sup> This mode is only active for crystallites of finite size and its intensity varies inversely with their diameter.<sup>50</sup> A remnant of this mode is in fact seen in the calculated Raman spectra of Beeman's 100%  $sp^2$  CRN,<sup>5</sup> suggesting that it can survive considerable disordering, and clearly the effects of various disorders should be studied further. So far, only the growth of this mode up to 500 °C has been studied.<sup>4</sup> One expects it to grow until about 1000 °C and then to decline as graphitization begins and the crystallites coalesce.

Wada *et al.*<sup>4</sup> found that the intensity of the disorder mode at 500 °C was consistent with  $\sim 20\text{-\AA}$  graphitic islands. They further observed  $\sim 3 \times 10^{19} \text{ cm}^{-3}$  of unpaired spins in their films and attributed them to dangling bonds at the edges of the islands. As they found that the spin concentration did not increase during annealing, whilst this usually peaks sharply during crystallization in  $a$ -Si or  $a$ -Ge because their dangling bonds mediate their crystallization, they proposed that  $\sim 20\text{-\AA}$  graphitic islands already existed in  $a$ -C and that annealing occurred by internal rearrangements within the islands, not involving dangling bonds.<sup>4</sup>

Much of this model is consistent with our results. We have seen how  $\pi$  bonding favors compact graphitic clusters. Islands of 15–20 Å possess 34–60 rings. This ring order is quite consistent with an experimental pseudogap of 0.4–0.7 eV,<sup>3,49,52,53</sup> as seen in Fig. 5, if one notes that the optical absorption edge is very broad (Fig. 6) and consequently the absorption at  $\alpha = 10^4 \text{ cm}^{-1}$  is controlled not

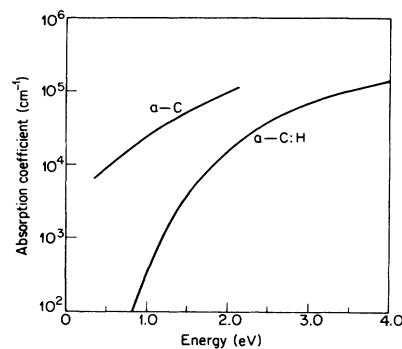


FIG. 6. Experimental optical-absorption spectra of typical samples of  $a$ -C (Ref. 3) and  $a$ -C:H (Ref. 59).

by clusters of average size but by the  $\sim 3\%$  of larger or less compact clusters. We differ from Wada *et al.*<sup>4</sup> in one respect; we suggest the clusters are interconnected by  $sp^3$  sites rather than surrounded by dangling bonds because (a) the observed number of spins is 2 orders of magnitude too small, and (b) dangling bonds are likely to be slightly mobile in resonantly bonded systems like  $a$ -C (see Sec. VI) so they may participate in crystallization without their density changing.

A question for a model based on 95%  $sp^2$  sites is why such sites should form islands at all rather than percolate entirely through the sample. In other words, why is strain relieved abruptly at the island edges rather than being distributed as a bond-angle disorder throughout the structure? We believe this occurs to maximize the  $\pi$  bonding energy. The interaction energy between neighboring  $\pi$  orbitals varies with dihedral angle as  $\cos\phi$ . The bonding energy gained by having almost all  $\pi$  orbitals aligned in islands ( $\phi \sim 0$ ) is then greater than that expected for a broad distribution of dihedral angles. A similar effect is seen, for instance, in  $a$ -Si, where rather than finding a broad distribution of bond lengths, the radial distribution function is sharply peaked at the crystalline nearest-neighbor bond length, with strain relieved via dangling bonds. The island edges then relieve strain in  $a$ -C in a similar manner to the latent dangling bonds in Phillips's model<sup>54</sup> for medium-range order in  $a$ -Si.

In detail, Phillips<sup>54,55</sup> noted that random networks with an average coordination of over 2.4 were overconstrained and would act to relieve strain by forming islands surrounded by intrinsic dangling bonds. He then proposed that the majority of these dangling bonds would reconstruct into weak bonds. A similar model is likely to be valid for  $a$ -C, modified to include the  $\pi$  bonding. In the  $a$ -C network, there are now two mechanisms to relieve strain, either by breaking  $\sigma$  bonds or by breaking  $\pi$  bonds. The latter mechanism requires less energy and only requires the presence of a periphery of either  $sp^2$  sites with  $\phi \sim 90^\circ$  or of  $sp^3$  sites without  $\pi$  states. Confining  $\pi$  bonding to islands relieves strain at their boundary and has the important effect of isolating the island's  $\pi$  electron states. The model does not predict the number of peripheral sites expected, but interestingly the probable concentration of  $sp^3$  sites in  $a$ -C ( $\sim 5\%$ ) is similar to that

of broken bonds in Phillip's model of *a*-Si ( $\sim 3.5\%$ ) (Ref. 54).

### V. PROPERTIES OF *a*-C:H

Although the hardness of *a*-C:H films was initially attributed to "diamondlike"  $sp^3$  bonding,<sup>56</sup> electron energy loss,<sup>7</sup> core-level spectroscopy,<sup>7</sup> nuclear magnetic resonance,<sup>9</sup> infrared spectroscopy,<sup>10,57</sup> and more detailed electron diffraction studies<sup>11</sup> quickly established that such films still contain a considerable proportion of  $sp^2$  sites. *a*-C:H also differs from *a*-Si:H in that the hydrogen content is typically much higher, 30–60% compared to 5–15%.<sup>9,10</sup> Annealing *a*-C:H in the range 400–600°C causes the films to lose hydrogen and gradually acquire the character of *a*-C, with its almost complete  $sp^2$  bonding.<sup>7</sup> Although hydrogen has clearly encouraged  $sp^3$  bonding, Dischler *et al.*<sup>10,57</sup> have found the hydrogen to bond to carbon  $sp^3$  and  $sp^2$  sites with similar probability, and this is supported by electron-energy-loss data.<sup>7</sup> We have, therefore, also calculated the local DOS of various H—C ( $sp^3$ ) and H—C ( $sp^2$ ) configurations (Fig. 7). It is immediately apparent from Figs. 2 and 7 that both C—C  $\sigma$  and C—H  $\sigma$  states lie at least 2.5 eV on either side of  $E_F$ . Clearly, therefore, the gap of *a*-C:H must also be controlled by the carbon  $\pi$  states.

The most surprising aspect of the optical gap of *a*-C:H is its small size. Experimentally, the  $E_{04}$  gap (at which the absorption coefficient equals  $10^4 \text{ cm}^{-1}$ ) lies in the 1.5–2.7-eV range.<sup>7–10,56–61</sup> Also, according to electron energy loss<sup>7</sup> and NMR,<sup>9</sup> a typical gap of  $\sim 2$  eV is achieved with only 30–40% of the carbon sites being  $sp^2$ .

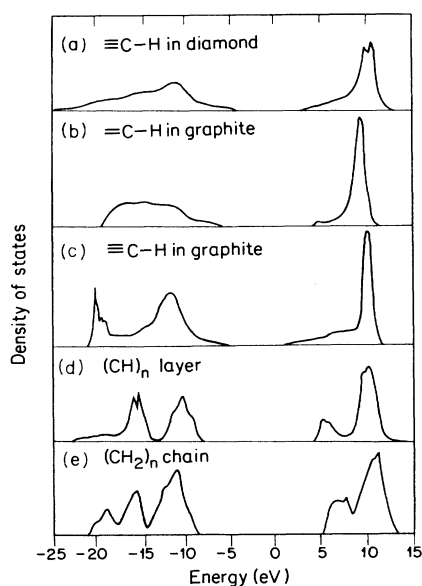


FIG. 7. Local DOS on the hydrogen sites for various hydrocarbon configurations: (a) a tetrahedral  $\equiv\text{C}-\text{H}$  site in diamond, (b) a planar  $=\text{C}-\text{H}$  site in graphite, (c) a tetrahedral  $\equiv\text{C}-\text{H}$  site in graphite, (d) a  $(\text{CH})_\infty$  layer of  $A7$  symmetry, and (e) a  $(\text{CH}_2)_\infty$  chain.

Thus, not only is it much less than a  $\sigma-\sigma^*$  gap, it is also much smaller than the  $\pi-\pi^*$  gap in the basic  $\pi$  systems, ethylene and benzene ( $E_g = 2\beta = 5.8$  eV for both theoretically, or 4.3 and 4.5 eV, respectively, experimentally for triplet transitions). Clearly, the remaining  $sp^2$  sites in *a*-C:H must be strongly clustered and the optical gap depends again on the medium rather than short-ranged order. From the results of Sec. III and Fig. 5, we estimate that this gap requires the clustering of  $sp^2$  sites as either four or more fused aromatic rings or as a polyene chain of six or more atoms, or as a quinoid configuration (8). The optical-absorption edge shown in Fig. 6 is again rather broad, implying that a large distribution of cluster sizes is again present, with the  $E_{04}$  gap again depending on the 1–5% of largest clusters. Even so, this is an extremely strong correlation of the remaining  $sp^2$  sites, and perhaps this accounts for the significant graphitic structural ordering still found in *a*-C:H by diffraction.<sup>11</sup> There is evidence from the dielectric function  $\epsilon_2$  that the predominant  $\pi \rightarrow \pi^*$  transition is at 5.3 eV, as in benzene,<sup>61</sup> suggesting that the most common  $sp^2$  cluster is a single sixfold ring. Finally, we remark again that the gap depends primarily on the  $sp^2:sp^3$  ratio and not explicitly on the H constant, and this is indeed found experimentally.<sup>9</sup>

We noted in Sec. III that the  $\pi$  spectrum is expected to be approximately symmetric about the gap center. This applies to both band states and localized states. Thus we expect the valence- and conduction-band tails to have roughly equal slopes and that  $E_F$  should remain near midgap, independent of the gap width. Experimentally, this is not really confirmed; Jones and Stewart<sup>58</sup> find that undoped *a*-C:H is *n* type with  $E_F$  above midgap, and as

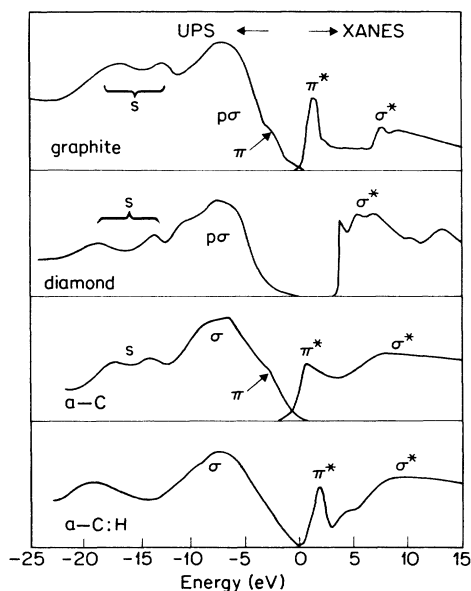


FIG. 8. Ultraviolet photoemission spectra (Ref. 39) and carbon 1s absorption spectra (XANES) (Ref. 7) of graphite, diamond, *a*-C, and *a*-C:H. The XANES spectra have been shifted in energy by 283 eV so as to model the conduction band density of states.

the gap varies,  $E_F$  tends to lie at a constant distance above  $E_v$ .

A third type of amorphous carbon can also be identified, prepared by ion-beam bombardment deposition methods such as magnetron sputtering,<sup>56,62-64</sup> and frequently called *i*-C. The ion bombardment during deposition appears to induce a greater proportion of  $sp^3$  sites in the films, which makes them harder. The films are usually of *i*-C:H, but recently unhydrogenated *i*-C has been prepared.<sup>63,64</sup> The analysis of the gap and the electronic structure of *i*-C:H follows that of *a*-C:H. For unhydrogenated *i*-C, Savvides<sup>63</sup> finds  $E_{04} \sim 0.5$  eV, similar to that of evaporated *a*-C, indicating that it again contains graphitic clusters of up to  $\sim 15$  Å across. However, its optical absorption below 8 eV is much weaker. These transitions correspond to only  $\pi \rightarrow \pi^*$  excitations, and indicates that the proportion of  $sp^2$  sites in *i*-C has declined. Furthermore, the minimally hydrogenated samples of Zelez<sup>64</sup> have  $E_{04} \sim 3$  eV, exceeding that of most *a*-C:H samples. This gap is very wide and suggests a remarkable reduction in clustering of the  $sp^2$  sites has occurred. Clearly, this material deserves more detailed study. Thus, *i*-C can contain a substantial proportion of  $sp^3$  sites, unlike other forms of pure *a*-C which we saw are only  $\sim 5\%$   $sp^3$ .

## VI. ELECTRONIC STRUCTURE AWAY FROM THE GAP

The valence- and conduction-band spectra of amorphous carbon films have been studied by photoemission and core-level spectroscopy. Some spectra are reproduced in Fig. 8. The valence-band spectrum of as-deposited *a*-C:H shows no hydrogen-related features,<sup>39,65</sup> presumably due to their low cross section, and little evidence of any  $\pi$  states near  $E_F$ . As *a*-C:H is annealed, it loses hydrogen and the  $\pi$  states become more apparent in the valence-band edge.<sup>39</sup> Interestingly, the  $s$  band develops a split peak feature around  $-16$  eV, characteristic of an even-membered ring structure and supporting the proposals of Sec. III that *a*-C consists of sixfold rings. The spectrum of unannealed *a*-C:H does not exhibit the splitting, because the  $sp^3$  bonding now dominates, and this type of bonding allows arbitrary ring statistics.

The carbon 1s XANES spectrum (Fig. 8) is very sensitive to the presence of empty  $\pi^*$  states in both molecules and solids.<sup>7,29</sup> These  $s \rightarrow \pi^*$  excitations produce a peak around 285 eV, below the onset of  $s \rightarrow \sigma^*$  transitions at  $\sim 289$  eV, seen respectively at 2 and 6 eV in Fig. 8. The  $s \rightarrow \pi^*$  absorption spectrum does not, however, directly reflect the  $\pi^*$  density of states because its lower edge is excitonically enhanced<sup>66,21</sup>—the graphite XANES spectrum peaks at 285 eV while the  $\pi^*$  DOS peaks at the  $M$  point,  $\sim 2.5$  eV above  $E_F$  (Figs. 2 and 8). Interestingly, the *a*-C spectrum decays more slowly above 285 eV than in graphite,<sup>7</sup> suggesting considerable disorder in the  $\pi^*$  states. The peak sharpens up again in hydrogenated samples and also shows a shoulder at  $\sim 287$  eV which Fink *et al.*<sup>7</sup> attributed to C—H  $\sigma^*$  states. Instead, we propose that in *a*-C:H the 285-eV peak corresponds to  $\pi^*$  states on fused rings and that the 287-eV shoulder is due to  $\pi^*$

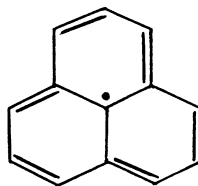
states on isolated C=C bonds, which lie higher above  $E_F$ . The  $s \rightarrow \pi^*$  transition is polarization dependent and has been studied in graphite.<sup>67</sup> It would be interesting to repeat this in *a*-C to discover if the films are truly isotropic.

In assessing the reliability of our tight-binding model, we note that tight binding was able to reproduce all the disorder-induced changes in the valence band of *a*-Si,<sup>12</sup> but was less convincing when applied to the conduction band, even the band-edge states. We expect tight binding to be equally good for the valence band of *a*-C, and now also to be valid for its  $\pi^*$  conduction band. This is because the  $\pi^*$  band retains local orbital character, while the  $\sigma^*$  states of Si are known to be delocalized, particularly at the  $X$  point. Thus, our results should reproduce the spectra of  $\sigma$ ,  $\pi$ , and  $\pi^*$  states with reasonable reliability. The nearest-neighbor (Hückel) model does overestimate some  $\pi$ - $\pi^*$  gaps slightly, but this is corrected when the second-neighbor term is included. A further improvement in results would follow from a full local orbital calculation, as in the work of Ching.<sup>68</sup> The Hückel model is much weaker when used for total energies, and it is difficult to estimate errors for this case. It is difficult to propose improvements as all simple tight-binding models of  $\sigma$  or  $\pi$  states fair worst on total energies. However, it is possible that the presence of medium-range order may allow  $k$ -space techniques to be employed using super-cell geometries.

## VII. DEFECT STATES

In this section we wish to deduce the origin of defect states in amorphous carbon, the states deep in the gap which control the transport and photoelectron properties of any amorphous semiconductor. The states are expected to arise from atoms with an atypical coordination. The amorphous semiconductors studied to date have been  $\sigma$  bonded and their gap states arise from changes in the  $\sigma$  coordination,<sup>12</sup> e.g., the dangling bond of *a*-Si:H and the valence alternation centers of *a*-As<sub>2</sub>Se<sub>3</sub>. In a system like amorphous carbon containing both  $\sigma$  and  $\pi$  bonding, there is in principle the possibility of both  $\sigma$  and  $\pi$  defects. Naturally though, as  $\pi$  bonding is weaker, we expect  $\pi$  defects to predominate due to their lower creation energy.

From the Hückel model of Sec. III, a  $\pi$  defect can be defined as a state with an energy near  $E = 0$ . We noted there that the  $\pi$  spectrum tends to be symmetric about  $E = 0$ . This implies that any cluster with an odd number of  $\pi$  orbitals will produce a state near  $E = 0$  and it will be half filled. The two simplest examples are the three-site olefinic chain, analogous to the allyl radical  $\text{CH}_2 \cdot \text{CH} \cdot \text{CH}_2$  and the cluster of three fused sixfold rings,



(13)



We concluded in Sec. III that odd-numbered clusters had a lower stability than even-numbered clusters. Thus, we may define the defect creation energy as

$$N_d = N(E_N - \bar{E}_N), \quad (14)$$

where  $N$  is the number of sites in the defect cluster,  $E_N$  is  $E_{\text{tot}}$  (the total  $\pi$  energy per site) for the cluster, and  $\bar{E}_N$  is the value of  $E_{\text{tot}}$  for an equivalent even cluster, read off from the trend line in Fig. 4. Figure 9 shows  $E_d$  for linear olefinic chains and for compact graphitic clusters. We see that  $E_d$  decreases rapidly with  $N$  for linear chains but it only decreases slowly and very unevenly for graphitic clusters.  $E_d$  for other configurations is found to lie between these two limits. There are two clear differences compared to  $\sigma$  defects. Firstly, there is no definable value of  $E_d$  for  $\pi$  defects, only a spectrum of values which could extend to  $E_d=0$  if sufficiently large clusters are present, whereas the dangling bond has a reasonably well-defined energy, of about half the  $\sigma$  bond energy. Secondly, the average energy of  $\pi$  defects is quite low, which is expected as  $\pi$  bonding is weaker than  $\sigma$  bonding. For instance, the maximum  $E_d$  for graphitic ( $\pi$ ) defects is  $\sim 0.4$  eV from Fig. 9, and this is significantly less than that of the dangling ( $\sigma$ ) bond (half the  $\sigma$  bond energy or  $\sim 1.8$  eV).

In general, the bonding configuration giving a defect state can best be determined from any hyperfine ESR spectrum. The hyperfine spectra of radicals in hydrocarbons arises mainly from the interaction of the unpaired electron with the nearby hydrogen nuclei, and this can be used to estimate the localization of the defect wave function. McConnell<sup>69</sup> found that the linewidth ( $a$ ) tends to be related to the localization of the  $\pi$  electron spin density on the adjacent carbon ( $\rho$ ) by

$$a = Q\rho, \quad (15)$$

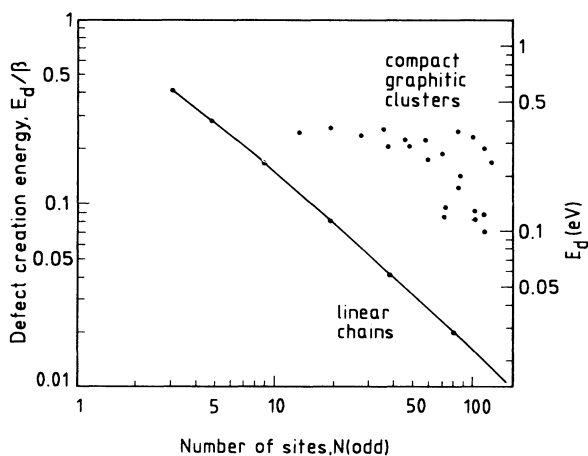


FIG. 9. Calculated dependence of defect creation energy  $E_d$  vs cluster size  $N$ , for linear chains and compact clusters of fused sixfold rings which form  $\pi$  defects. Numerical estimates are also included, using  $\beta = -1.4$  eV.

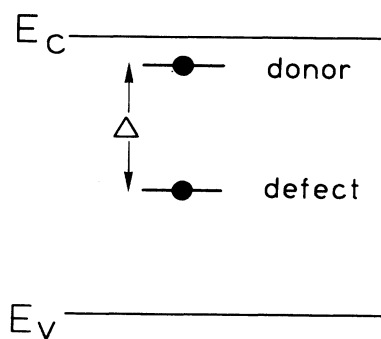


FIG. 10. Schematic energy levels in a compensated semiconductor.

with  $Q = -23$  G. In fact,  $\pi$  defects are expected to be quite delocalized; the defect state of the allyl radical extends over all three sites and that of (13) extends over all the exterior sites.

In a mixed  $\sigma, \pi$  bonded system like amorphous carbon, the  $\sigma$  defect, the dangling bond, must be defined as an *isolated* threefold coordinated site. In fact, we believe this defect will still be  $\pi$ -like in  $a$ -C:H. This is because the analogous molecular radical, the methyl radical  $\text{CH}_3$ , is planar not pyramidal,<sup>32</sup> so the unpaired electron is in a  $\pi$  orbital. Thus, we believe the dangling bond is  $\pi$ -like in  $a$ -C:H, and not  $sp^3$ -like as in  $a$ -Si:H.

Experimentally, the defect states of  $a$ -C form a continuous distribution across its pseudogap and these allow conduction by variable range hopping.<sup>3,70-72</sup> A spin density of  $\sim 10^{18} \text{ cm}^{-3}$  is found.<sup>4,73</sup> Assuming that such defects are associated with graphitic islands with an odd

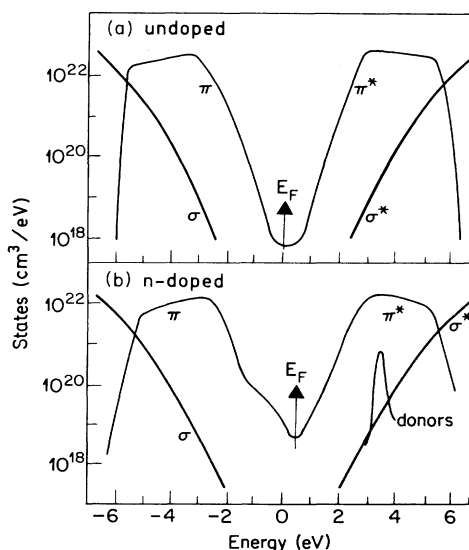


FIG. 11. Schematic density of gap states for (a) undoped and (b)  $n$ -type  $a$ -C:H.

number of sites, then only  $\sim 1\%$  of all islands are odd. This emphasizes how *a-C*, like all amorphous semiconductors, arranges its bonding to favor paired spins.

Hydrogenation decreases the number of spins to  $\sim 10^{16} \text{ cm}^{-3}$  in good samples, comparable to that in *a-Si:H*,<sup>73</sup> and generally spin densities in the range  $10^{16}$ – $10^{18} \text{ cm}^{-3}$  are found.<sup>74–78</sup> The low thermopower in *a-C:H* indicates transport quite close to  $E_F$ ,<sup>79</sup> so we suspect that defect states form a continuous distribution across the gap here too.

The correlation between defect creation energy and cluster size (Fig. 9), and between cluster size and band gap (Fig. 4) implies that the defect density in *a-C:H* will correlate inversely with optical gap. This is certainly found experimentally in that *a-C:H* deposited at higher temperatures usually has less H, a smaller gap, and more gap states. We therefore propose that hydrogenation lowers the defect density not by saturating dangling bonds, as in *a-Si:H*, but by reducing cluster sizes and thereby increasing the defect creation energy and decreasing their thermodynamic probability.

### VIII. DOPING

As *a-C:H* is one of the few amorphous semiconductors which may be substitutionally doped by group-III and -V elements, it is important to understand the underlying bonding mechanism, particularly in view of the substantial coordination disorder present in the host. Meyerson and Smith<sup>2</sup> discovered doping in *a-C:H*, and observed the thermopower sign reversal between *n*- and *p*-type doping which suggested that a substitutional mechanism was responsible.<sup>79</sup> Jones and Stewart<sup>58</sup> in their study emphasized that the doping efficiency was much lower than in *a-Si:H*, and this suggests that a substitutional mechanism may not be involved.

We argue first that doping in *a-C:H* is indeed substitutional, but strongly compensated. In *a-C:H* nitrogen and phosphorus dope with similar efficiencies,<sup>58</sup> while in *a-Si:H* nitrogen doping is exceedingly inefficient compared to phosphorus doping.<sup>80</sup> It has been argued that nitrogen atoms usually do not dope *a-Si:H* because they are too small to accommodate the necessary four Si neighbors.<sup>81</sup> However, we argue that nitrogen can form substitutional sites in *a-C:H* because it can now accommodate four of the smaller carbon atoms as neighbors. Thus, we believe the observation of substantial nitrogen doping supports a substitutional mechanism of *a-C:H*. It is also possible that group III and V provide some doping effect at three-fold sites, provided they are planar; for instance, boron is able to dope graphitized carbon.<sup>82</sup>

We argue secondly that the low doping efficiency in *a-C:H* is due to a strong autocompensation, in which doping is accompanied by an increased defect density. The basic idea of compensation applies equally to any semiconductor, crystalline or amorphous<sup>83</sup> (Fig. 10). In a *n*-type sample, if a donor electron can fall into a defect level lower in the gap, it gains an energy  $\Delta$ . If  $\Delta$  exceeds the defect creation energy  $E_d$ , defects will be spontaneously

created during deposition and trap the electrons, causing compensation. It is now known that *a-Si:H* is moderately compensated with  $\sim 90\%$  of carriers trapped in defect levels.<sup>84</sup> In *a-C:H*, we believe the relatively low  $E_d$  of  $\pi$ -like defects shown in Fig. 9, particularly of any large  $\pi$  clusters, results in greater compensation than in *a-Si:H*, and a much lower doping efficiency.

In summary, Fig. 11 shows a schematic density of states for *a-C:H*. The states of undoped *a-C:H* consist of widely separated  $\sigma$  and  $\sigma^*$  bands, between which lie the  $\pi$  and  $\pi^*$  bands, leaving a pseudogap say 2-eV wide and with a midgap density of states of  $10^{18} \text{ eV}^{-1} \text{ cm}^{-3}$  or lower. *N*-type doping introduces fourfold substitutional sites which create bound states below the  $\sigma^*$  band. Compensation increases the density of gap states and these merge with the valence-band tail so  $E_F$  only moves upwards by 0.2–0.5 eV.

### IX. CONCLUSIONS

This paper has discussed the bulk electron states, the structure, the defects, and the doping mechanism of various types of amorphous carbon. The band gap and total energy was analyzed for various configurations of  $sp^2$  and  $sp^3$  sites. It was found that the mere presence of  $sp^3$  sites was insufficient to produce an optical gap. The total energy of the  $\pi$  electrons favor the  $sp^2$  sites to be organized in compact clusters of fused sixfold rings which also maximizes the band gap. The band gap is found to vary roughly inversely with cluster size. These observations were used to confirm that evaporated amorphous carbon consists of  $\sim 95\%$   $sp^2$  sites with significant medium-range order, in the form of disordered graphite islands up to 15 Å in diameter. Turning to *a-C:H*, we confirmed that both band edges are still due to  $\pi$  states, and the size of the gap signifies that some of the  $\sim 30\%$  of its remaining  $sp^2$  sites must also be clustered, e.g., up to four fused sixfold rings. The band structures of various model structures of *a-C* and *a-C:H* were used to interpret their photoemission, optical and XANES spectra. The XANES spectra were shown to be particularly useful and sensitive to the presence of any  $sp^2$  sites.  $sp^3$  sites are more difficult to detect; NMR can be used in *a-C:H*, but not in *a-C* where it is most needed. Thus, there is no direct unambiguous means to detect  $sp^3$  sites in *a-C*. Our calculations, however, do support the use of  $\epsilon_2$  and the optical sum rule for this purpose. The defects of amorphous carbon were shown to be  $\pi$ -like states and to have a range of creation energies. It is argued that doping of *a-C:H* does occur by a substitutional mechanism, but with strong autocompensation due to the relatively low defect creation energy.

*Note added in proof.* Calculations by Bredas and Street<sup>85</sup> have reached similar conclusions to us concerning the origins of the optical gap.

### ACKNOWLEDGMENTS

The authors are grateful for conversations with D. Beeman and D. Jones. This paper is published with the permission of the Central Electricity Generating Board.

- <sup>1</sup>L. Holland and S. M. Ojha, *Thin Solid Films* **38**, L17 (1976).
- <sup>2</sup>B. Meyerson and F. W. Smith, *Solid State Commun.* **34**, 531 (1980).
- <sup>3</sup>J. J. Hauser, *J. Non-Cryst. Solids* **23**, 21 (1977).
- <sup>4</sup>N. Wada, P. J. Gaczi, and S. A. Solin, *J. Non-Cryst. Solids* **35**, 543 (1980).
- <sup>5</sup>D. Beeman, J. Silverman, R. Lynds, and M. R. Anderson, *Phys. Rev. B* **30**, 870 (1984).
- <sup>6</sup>D. F. R. Mildner and J. M. Carpenter, *J. Non-Cryst. Solids* **47**, 391 (1982).
- <sup>7</sup>J. Fink, T. Muller-Heinzerling, J. Pflugler, A. Bubenzer, P. Koidl, and G. Crecelius, *Solid State Commun.* **47**, 687 (1983).
- <sup>8</sup>D. A. Anderson, *Philos. Mag.* **35**, 17 (1977).
- <sup>9</sup>S. Kaplan, F. Jansen, and M. Machonkin, *Appl. Phys. Lett.* **47**, 750 (1985).
- <sup>10</sup>B. Dischler, A. Bubenzer, and P. Koidl, *Appl. Phys. Lett.* **42**, 636 (1983).
- <sup>11</sup>D. R. McKenzie, L. C. Botten, and R. C. McPhedran, *Phys. Rev. Lett.* **51**, 280 (1983).
- <sup>12</sup>For example, see J. Robertson, *Adv. Phys.* **32**, 361 (1983).
- <sup>13</sup>D. Weaire, *Phys. Rev. Lett.* **26**, 1541 (1971).
- <sup>14</sup>E. P. O'Reilly, J. Robertson, and D. Beeman, *J. Non-Cryst. Solids* **77**, 83 (1985).
- <sup>15</sup>G. S. Painter and D. E. Ellis, *Phys. Rev. B* **1**, 4747 (1970).
- <sup>16</sup>R. F. Willis, B. Fitton, and G. S. Painter, *Phys. Rev. B* **9**, 1920 (1974).
- <sup>17</sup>G. S. Painter, D. E. Ellis, and A. R. Lubinsky, *Phys. Rev. B* **4**, 3610 (1970).
- <sup>18</sup>C. D. Clark, P. J. Dean, and P. V. Harris, *Proc. R. Soc. London, Ser. A* **227**, 312 (1964).
- <sup>19</sup>F. J. Himpel, J. F. van der Veen, and D. E. Eastman, *Phys. Rev. B* **22**, 1967 (1980).
- <sup>20</sup>W. Eberhardt, I. T. McGovern, E. W. Plummer, and J. E. Fischer, *Phys. Rev. Lett.* **44**, 200 (1980).
- <sup>21</sup>J. Robertson, *Phys. Rev. B* **29**, 2131 (1984).
- <sup>22</sup>B. B. Pate, P. M. Stefan, C. Binns, P. J. Jupiter, M. L. Shek, I. Lindau, and W. E. Spicer, *J. Vac. Sci. Technol.* **19**, 349 (1981).
- <sup>23</sup>W. A. Harrison, *J. Vac. Sci. Technol. B* **3**, 1231 (1985).
- <sup>24</sup>R. C. Tatar and S. Rabii, *Phys. Rev. B* **25**, 4126 (1982).
- <sup>25</sup>M. Posternak, A. Baldereschi, A. J. Freeman, E. Wimmer, and M. Weinert, *Phys. Rev. Lett.* **50**, 430 (1983).
- <sup>26</sup>Th. Fauster, F. J. Himpel, J. E. Fischer, and E. W. Plummer, *Phys. Rev. Lett.* **51**, 430 (1983).
- <sup>27</sup>R. K. Nesbet, *J. Chem. Phys.* **32**, 1114 (1960).
- <sup>28</sup>R. G. Cavell, S. P. Kowalezyk, L. Ley, R. A. Pollak, B. Mills, D. A. Shirley, and W. Perry, *Phys. Rev. B* **7**, 5313 (1973).
- <sup>29</sup>W. Eberhardt, R. P. Haelbich, M. Iwan, E. E. Koch, and C. Kunz, *Chem. Phys. Lett.* **40**, 180 (1976).
- <sup>30</sup>R. Haydock, in *Solid State Physics*, edited by H. Ehrenreich (Academic, New York, 1980), Vol. 35, p. 215.
- <sup>31</sup>E. P. O'Reilly and J. Robertson, *Phys. Rev. B* **27**, 3780 (1983).
- <sup>32</sup>A. Streitwieser and C. H. Heathcock, *Introduction to Organic Chemistry* (MacMillan, London, 1976).
- <sup>33</sup>L. Salem, *Molecular Orbital Theory of Conjugated Polymers* (Benjamin, New York, 1966).
- <sup>34</sup>R. Hoffman, *Tetrahedron* **22**, 521 (1966).
- <sup>35</sup>K. S. Pitzer and E. Clementi, *J. Am. Chem. Soc.* **21**, 4477 (1959).
- <sup>36</sup>D. Weaire and N. Rivier, *Contemp. Phys.* **25**, 59 (1984).
- <sup>37</sup>W. A. Harrison, *Electronic Structure* (Freeman, San Francisco, 1979).
- <sup>38</sup>F. R. McFreely, S. P. Kowalezyk, R. G. Cavell, R. A. Pollak, and D. A. Shirley, *Phys. Rev. B* **9**, 5263 (1974).
- <sup>39</sup>D. Wesner, S. Krummacher, R. Carr, T. K. Sham, M. Strongin, W. Eberhart, S. L. Weng, G. Williams, M. Howells, F. Kampas, S. Heald, and F. W. Smith, *Phys. Rev. B* **28**, 2152 (1983).
- <sup>40</sup>R. E. Franklin, *Acta Crystallogr.* **3**, 107 (1950).
- <sup>41</sup>J. Kakinoki, K. Katada, T. Hanawa, and T. Ino, *Acta Crystallogr.* **13**, 171 (1960); **13**, 448 (1960).
- <sup>42</sup>T. Noda and M. Inagaki, *Bull. Chem. Soc. Jpn.* **37**, 1534 (1964).
- <sup>43</sup>B. T. Boiko, L. S. Palantik, and A. S. Derevyanchenki, *Dok. Akad. Nauk SSSR* **179**, 316 (1968) [*Sov. Phys.—Dokl.* **13**, 237 (1968)].
- <sup>44</sup>B. J. Stenhouse, and P. J. Grout, *J. Non-Cryst. Solids* **27**, 247 (1978).
- <sup>45</sup>A. Oberlen, M. Oberlen, and M. Maubois, *Philos. Mag.* **32**, 833 (1975).
- <sup>46</sup>S. Ergun, *Acta Crystallogr. A* **29**, 605 (1973).
- <sup>47</sup>J. Lannin, in *Amorphous and Liquid Semiconductors*, edited by W. E. Spear (Council for Consultancy and Liaison, Edinburgh, 1977), p. 110.
- <sup>48</sup>R. O. Dillon, J. A. Woollam, and V. Katkanant, *Phys. Rev. B* **29**, 3482 (1984).
- <sup>49</sup>J. Knoll and J. Geiger, *Phys. Rev. B* **29**, 5651 (1984).
- <sup>50</sup>F. Tuinstra and J. L. Koenig, *J. Chem. Phys.* **53**, 1126 (1970).
- <sup>51</sup>R. J. Nemanich and S. A. Solin, *Phys. Rev. B* **20**, 392 (1979).
- <sup>52</sup>E. T. Arakawa, U. W. Williams, and T. Inagaki, *J. Appl. Phys.* **48**, 3176 (1977).
- <sup>53</sup>G. Jungk and C. H. Lange, *Phys. Status Solidi B* **50**, K71 (1972).
- <sup>54</sup>J. C. Phillips, *Phys. Rev. Lett.* **42**, 1151 (1979).
- <sup>55</sup>M. F. Thorpe, *J. Non-Cryst. Solids* **57**, 355 (1983).
- <sup>56</sup>C. Weissmantel, *Thin Solid Films* **58**, 101 (1979).
- <sup>57</sup>B. Dischler, A. Bubenzer, and P. Koidl, *Solid State Commun.* **48**, 105 (1983).
- <sup>58</sup>D. I. Jones and A. D. Stewart, *Philos. Mag. B* **46**, 423 (1982).
- <sup>59</sup>F. W. Smith, *J. Appl. Phys.* **55**, 764 (1984).
- <sup>60</sup>D. R. McKenzie, R. C. McPhedran, N. Savvides, and L. C. Botten, *Philos. Mag. B* **48**, 341 (1983).
- <sup>61</sup>J. Fink, T. Muller-Heinzerling, J. Pflugler, B. Scheerer, B. Dischler, P. Koidl, A. Bubenzer, and R. E. Sah, *Phys. Rev. B* **30**, 4713 (1984).
- <sup>62</sup>C. Weissmantel, K. Bewilogua, A. K. Breuer, D. Dietrich, U. Ebersbach, H. J. Erler, B. Rau, and G. Risse, *Thin Solid Films* **96**, 31 (1982); C. Weissmantel, *Thin Solid Films* **92**, 55 (1982).
- <sup>63</sup>N. Savvides, *J. Appl. Phys.* **59**, 4133 (1984).
- <sup>64</sup>J. Zelez, *J. Vac. Sci. Technol. A* **1**, 306 (1983).
- <sup>65</sup>P. Oelhafen, J. L. Freehouf, J. M. Harper, and J. J. Cuomo, *Thin Solid Films* **120**, 231 (1984).
- <sup>66</sup>E. J. Mele and J. J. Risko, *Phys. Rev. Lett.* **43**, 68 (1979).
- <sup>67</sup>R. A. Rosenberg, P. J. Love, and V. Rehn, *Phys. Rev. B* **33**, 4034 (1986).
- <sup>68</sup>W. Y. Ching, D. J. Lam, and C. C. Lin, *Phys. Rev. B* **21**, 2378 (1980).
- <sup>69</sup>H. M. McConnell, *J. Chem. Phys.* **28**, 1188 (1958).
- <sup>70</sup>C. J. Adkins, S. M. Freake, and E. M. Hamilton, *Philos. Mag.* **22**, 183 (1970).
- <sup>71</sup>M. Morgan, *Thin Solid Films* **7**, 313 (1971).
- <sup>72</sup>R. Grigorvici, A. Devenyi, A. Gheorghiu, and A. Belu, *J. Non-Cryst. Solids* **8**, 793 (1972).
- <sup>73</sup>F. Jansen, M. Machonkin, S. Kaplan, and S. Hark, *J. Vac. Sci. Technol. A* **3**, 605 (1983).
- <sup>74</sup>R. J. Gambino and J. A. Thompson, *Solid State Commun.* **34**, 15 (1970).

- <sup>75</sup>D. J. Miller and D. R. McKenzie, *Thin Solid Films* **108**, 257 (1983).
- <sup>76</sup>I. Watanabi and T. Okumura, *Jpn. J. Appl. Phys.* **24**, L122 (1985).
- <sup>77</sup>I. Watanabi, S. Hasegawa, and Y. Kurata, *Jpn. J. Appl. Phys.* **21**, 856 (1982).
- <sup>78</sup>S. H. Lin and B. J. Feldman, *Philos. Mag. B* **47**, 113 (1983).
- <sup>79</sup>B. Meyerson and F. W. Smith, *Solid State Commun.* **41**, 23 (1982).
- <sup>80</sup>B. Dunnett, D. I. Jones, and A. D. Stewart, *Philos. Mag. B* **53**, 159 (1986).
- <sup>81</sup>J. Robertson, *J. Non-Cryst. Solids* **77**, 37 (1985).
- <sup>82</sup>S. Mrozowski, *Carbon* **9**, 97 (1971).
- <sup>83</sup>J. Robertson, *Phys. Rev. B* **33**, 4399 (1986).
- <sup>84</sup>M. Stutzmann and R. A. Street, *Phys. Rev. Lett.* **54**, 1836 (1985).
- <sup>85</sup>J. L. Bredas and G. B. Street, *J. Phys. C* **18**, L651 (1985).